



**Fermi National Accelerator Laboratory**

**FERMILAB-Pub-90/152-E**  
**[E-735]**

## **A Scintillator Hodoscope at the Tevatron Collider \***

**E. W. Anderson, C. S. Lindsey and C. H. Wang**  
*Iowa State University*  
*Ames, Iowa 50011*

**C. Hojvat, D. Reeves and F. Turkot**  
*Fermi National Accelerator Laboratory*  
*P. O. Box 500*  
*Batavia, Illinois 60510*

**July 1990**

\* Submitted to Nucl. Instrum. Methods A.



**Operated by Universities Research Association Inc. under contract with the United States Department of Energy**

## **A Scintillator Hodoscope at the Tevatron Collider**

E.W. Anderson, C.S. Lindsey\* and C. H. Wang  
*Iowa State University, Ames, Ia. 50011, USA*

C. Hojvat, D. Reeves and F. Turkot  
*Fermilab\*\*, Batavia Il. 60510, USA*

A plastic scintillator hodoscope for an experiment at the Fermilab Tevatron proton-antiproton Collider is described. The hodoscope is used on-line to form a charged multiplicity trigger and off-line to study charged particle multiplicity distributions. The hodoscope consists of 240 counters covering the pseudorapidity range of  $\pm 3.25$ . It is designed to survive a radiation dose of up to 100krad over the experiment's lifetime.

### **1. Introduction:**

A hodoscope has been built and used in experiment E735 at the Tevatron proton-antiproton Collider at Fermilab. E735 is designed to search for evidence in proton-antiproton collisions of the formation of the quark-gluon plasma phase of matter predicted by quantum chromodynamics [1]. Transition to a quark-gluon plasma requires very high energy density ( $>2\text{GeV/fm}^2$ ). Assuming the energy density is proportional to the charged particle multiplicity [2], events with high charged particle multiplicities (e.g.  $N_C=50-200$ ) are of primary interest. Since the data acquisition system cannot accept all events from a minimum bias trigger, a trigger system was designed that could select events on-line according to their multiplicities. A hodoscope consisting of an array of 240 scintillation counters surrounds the interaction point. A charged particle traversing a counter's plastic scintillator produces a fast signal that constitutes a "hit". The trigger processor system [3] uses the number of hodoscope hits to decide whether to accept the event for the data acquisition system.

The Collider tunnel environment includes background radiation from beam interactions with residual gas and from stray beam particles interacting with the beampipe and surrounding materials. The tunnel and

E735 experimental area contain both the Collider beams and the Main Ring (MR) beam. The latter accelerates protons about every 3s for the production of antiprotons. The largest background radiation contribution comes from the MR, especially during the injection and acceleration of the beam. The hodoscope scintillator, photomultiplier tubes (PMT) and bases have to perform in these high rate backgrounds and survive a cumulative radiation dose of up to 100krad over the experiment's lifetime. This paper describes the design of the hodoscope counter array to meet these requirements and reports the hodoscope's performance over two running periods of the Collider.

## 2. E-735 Experiment

The experimental setup of E735 has been described previously [4]. Fig. 1 shows two views of the apparatus in the C0 interaction hall at the Collider. The setup is divided into essentially two parts: (1) a central detector system located around the beam collision point, and (2) a magnetic spectrometer to the side. The central detectors determine the total charge multiplicity from tracking chambers and the hodoscope counters. Approximately half of the particles produced in the interaction are included in the central detectors' acceptance. The magnetic spectrometer (covering 0.5sr solid angle and consisting of a magnet, tracking chambers, and time of flight counters) tracks and momentum analyzes those charged particles at angles nearly normal to the beampipe.

The time of flight (TOF) system gives particle identification for charge particles ( $\pi^\pm, K^\pm, p$  and  $\bar{p}$ ) in the spectrometer up to 1.5GeV/c [4]. The interaction time is determined by the upstream and downstream (as defined by the proton direction) TOF trigger counters ( $p\bar{p}$  counters). The signals from these counters are required by the trigger logic to be in coincidence with the beam-crossing timing (derived from the accelerator rf system) to minimize out-of-time background events.

In the central region, a cylindrical "Central Tracking Chamber" (CTC) surrounds the collision point and a planar vertex chamber lies between the beampipe and the inner CTC wall. The "Barrel" hodoscope array surrounds the outer wall of the CTC. Upstream and downstream of the collision point are the endcap tracking chambers, the endcap hodoscopes, and finally the  $p\bar{p}$  counters.

The number of hits in the hodoscope gives a fast indication (i.e. within a few hundred ns, with beam crossings occurring every 3 $\mu$ s) of the event multiplicity for the trigger decision. The CTC and endcap tracking chambers, as well as the hodoscope, determine off-line the charged multiplicity within a pseudorapidity range of  $|\eta| < 3.25$ . The spectrometer examines particles from the central part of the collision within  $40^\circ < \theta < 110^\circ$  and  $0^\circ < \phi < 20^\circ$ . Transverse momenta and mass identified particle ratios can then be studied as a function of the charged multiplicity to search for predicted signals of quark-gluon plasma formation.

### 3. Design Considerations

In the E735 experimental area both the Collider and its proton abort beamlines are contained in a single beampipe. The MR and its abort beamlines are in separate beampipes and pass just above the hodoscope.

To accumulate antiprotons for the Collider, protons are accelerated in the MR from 8GeV to 120GeV and extracted towards the anti-proton production target. Antiprotons from the target are cooled and stored in the Accumulator for later transfer to the Collider. The process is repeated every 3s. Figure 2 shows the MR acceleration cycle and typical hit rates produced by MR background radiation at C0. The backgrounds are especially high during the MR acceleration. Losses from the Collider beams are much lower than from the MR since the Collider remains mostly in a stable colliding mode at a fixed energy. Loss detectors at C0 are monitored to minimize the backgrounds with adjustments to the beams. However, the total dose (as measured both by the loss detectors and by thermoluminescent detectors [5] placed at different points on the detector) over two running periods reached about 65krad for the counters nearest to the MR (versus 1 to 2krads for counters farthest from it).

To meet both radiation hardness and mechanical constraints in the central detector region, the hodoscope had to fulfill the following requirements: (1) the plastic scintillator and light guides must not degrade substantially for doses less than 100krads; (2) the PMT's must be protected from large currents that could exceed their rated values and damage the tubes; (3) the components of the PMT bases must be radiation hard; (4) the hodoscope must cover as much as possible of the total solid

angle, yet be highly segmented to give a good indication of the charged multiplicity and fit within the space below the MR beampipes; (5) the amount of material intervening between the collision vertex and the scintillator must be minimized to reduce the production of secondary particles; and (6) the PMT's must be protected from the stray fields of the spectrometer magnet .

#### **4. Hodoscope Design**

Figures 3-6 show diagrams of the 3 hodoscope parts: the barrel plus the upstream and downstream endcaps.

The barrel hodoscope, fig. 3, consists of 96 counters arranged in two 48 counter sections upstream and downstream of the interaction point. The counters are arranged in slats (5.4cm wide, 97cm long and 0.635cm thick) running parallel to the beampipe and each spanning  $7.5^\circ$  in azimuth. A prism at one end reflects light into the PMT. The counters are at a radius of 42.4cm from the beam line and span  $\pm 1.6$  units of pseudorapidity. Six counters were shortened to reduce the material traversed by particles entering the spectrometer (see fig. 1b and fig. 3). This spectrometer window reduced the total hodoscope solid angle coverage by about 2%. Fig. 4 shows a design of a single barrel counter assembly. The counters are mounted on two Al rings which also support the CTC.

As seen in fig. 1, some of the barrel counters are quite close to the spectrometer magnet. For the closest PMT's the field reaches 1kG normal to the tube and 100G parallel to the tube. Tests in a magnet showed that the tubes could be protected with a combination of a thin high permeability metal tube [6] inside a 0.635cm thick Fe tube, 25cm long and 5cm in diameter. This arrangement gave no gain decrease for fields up to  $B$  transverse  $< 1\text{kG}$  and  $B$  parallel  $< 500\text{G}$ .

The Fe shields are also used in the structural support of the counters. Figure 4 shows the barrel counters supported at each end by tabs extending from the shields to the support rings. The Fe shield is strapped to an Al U-channel while the scintillator underneath is attached to the channel with tape. The end support rings are on bearings that allow the entire barrel assembly (with the CTC) to be rotated for installation, access and removal of individual counters.

Figures 5 and 6 show an endcap hodoscope (the upstream and

downstream endcaps are mirror images of one another). The endcap is divided into 3 rings of 24 counters each. Fig. 6 shows a cutaway of the endcaps showing the 3 types of counters in the rings. Each counter spans about 0.5 units of pseudorapidity and  $15^\circ$  in azimuth. The counters are mounted on a sandwich structure of 0.8mm G-10 and styrofoam, which minimizes the amount of material traversed by particles from the interaction. An Al outer rim at a radius of 66cm supports the counters. The entire structure is separable into 3 wedges. It sits on a rotatable base that allows each wedge to be installed or removed one at a time. The individual counters are mounted to support arms by tabs on the iron shields. This design, with the PMT's and shields as far from the beampipe as possible, minimizes the amount of material between the interaction point and the  $p\bar{p}$  counters.

### **5. Photomultiplier Tubes and Bases**

The PMT used for all hodoscope counters is the 28.5mm diameter, 10 stage Hamamatsu 1398 tube with UV glass window [7]. It has a 2ns risetime with a gain of  $6 \times 10^6$  at 1.5kV. The maximum HV is 1900v and the maximum recommended average anode current is 200 $\mu$ A. The PMT's used were preselected by Hamamatsu to have gain variations within a factor of 2. The PMT's were run in grounded anode mode with the anode signal connected via RG8 (foam) 50 $\Omega$  cables to a transformer splitter [8]. One splitter output was used for pulse height analysis and another output went to a discriminator with a threshold of 30mV. The discriminator outputs went to the trigger processor, time to digital converters and scalars.

To insure maximum lifetime, the PMT's had to be protected from high currents during the periods of high MR backgrounds (see fig. 2). Two candidate bases were considered: (1) a high current (1mA) resistor base with a switch to short dynodes 1 and 2 to decrease the PMT gain during periods of high MR losses; and (2) a low current (200 $\mu$ A) resistor base, fig. 7, that could not exceed the PMT maximum current (fig. 2c). Transistor bases were rejected due to their susceptibility to radiation damage (one was used briefly to determine the maximum rates, fig. 2b).

With the low current base the PMT gain began to sag with the order of

10 minimum ionizing particles traversing the counter simultaneously. The switch base did not sag but could not be made sufficiently reliable. The low current design was chosen for the full hodoscope. The detector trigger was gated off during the MR loss period so that the low current base gain loss did not affect the data recorded. The gate was extended about 50 $\mu$ s beyond the loss period to allow for high-voltage recovery.

## **6. Scintillator and Light Guides**

A study was performed on the effects of the C0 background radiation on several types of plastic scintillators [9]. The polyvinyltoluene (PVT) based Bicron BC-408 [10] light output degraded by as much as 50% for doses of around 60krad. However, it was found to be superior to acrylic scintillator and to a polystyrene based scintillator, and all hodoscope counters were built of this material. At the beginning of the experiment the counters were efficient for minimum ionizing tracks at several hundred volts below the maximum value recommended for the PMT's. So an increase in gain of a factor of two or three was available to compensate for scintillator degradation.

The radiation affected primarily the light producing fluor in the scintillator rather than the PVT matrix [9]. Since acrylic light guides darken dramatically from even modest doses, pure PVT with no scintillation fluor additive was chosen as the light guide material. In addition, a quencher chemical (benzyl-phenone) of 1% was included by Bicron to diminish the natural scintillation of the PVT.

The PVT was saw cut to a rough shape, machined to final form with a diamond fly cutter and then hand-polished. Curved light guides were bent by warming the PVT, while the ends remained at room temperature. When softened they were laid over a form and allowed to cool. Surface crazing developed occasionally after a few days in the areas between the heated and cool sections. The crazing was removed by heat annealing the affected area. All counters were wrapped in Al foil and covered with opaque paper.

For both the barrel and outer endcap ring counters, a prism was used in the light guides to reflect light through 180 degree bends to obtain compact designs (fig. 4 and 6). The light transmission of 70% of a curved (radius of 3cm) light guide was found adequate.

## **7. Light Pulser**

The counter pulse height distributions were continuously monitored during data taking. In addition, a light pulser testing system was implemented and used primarily when no beam was available. Light from a xenon flashtube was directed into a bundle of 380 $\mu$ m plastic clad light fiber with 200 $\mu$ m silica core [11] (pure silica core was reported to be less susceptible to radiation damage than other types of fibers [12]). The fibers were cut to 30m lengths and were individually strung through 3.2mm plastic tubing for protection. The fibers traveled from the experiment's control room to the detectors and were connected to the counters as shown in fig. 8. A small prism with a hole drilled into it was glued to the face of the scintillator and a 1.6mm black tube was glued into this hole. The light fiber was introduced into the smaller tube, with the fiber protecting tube slipped over the smaller tube to make a light tight connection. The fiber tube was then held in place by a plastic hold-down.

## **8. Performance of the Hodoscope**

During the two Collider runs of 1987 and 1988-89 we experienced less than 1% PMT failures. The 4 month run in 1987 resulted in an accumulated dose of 25krad in the highest radiation region to a few hundred rads for counters farthest from the MR. The average pulse height decrease (as measured by the position of the minimum ionizing peaks in the pulse height distributions) was less than 10% and all working counters remained efficient. In the 1988-1989 run of 12 months, the accumulated dose was about 40krads in the maximum region to about 1 krad farthest from the MR. Gains dropped from 10%-50% over the course of the run and some counters needed increases in HV to remain efficient. (Some recovery of the scintillator light output may have occurred in the period between the two runs when the hodoscope was removed from the tunnel for 1 year. See ref. [9] for discussion of scintillation light output recovery in Bicron BC-408).

After the first Collider run, some of the counters were inspected for radiation damage. The scintillator showed no visible discoloration; the light guides, however, showed some darkening. Fig. 9 shows the



measurements of transmission vs wavelength of two 2.54cm thick pieces of PVT light guides, one from an exposed (25krad) counter and one unexposed. At the shorter wavelengths there is clear degradation. However, the sensitivity of the tubes to the longer wavelengths has apparently prevented any substantial decrease in the counter efficiency. A possibility is that the quenching additive is affected by the radiation and caused the observed darkening.

Using the trigger processor [3] the number of lower multiplicity events written to tape was scaled down in favor of the more interesting high multiplicity events. The average luminosity of the Collider in 1988-1989 increased by almost a factor of 10 over the 1987 run. Yet, using the trigger processor, we were able to maintain the data acquisition live time at 80-90% and remain sensitive to the very high multiplicity events.

The hodoscope system was also used in rejecting background events caused by beam interactions with residual gases in the beam pipe or by stray beam particles hitting the beampipe. These events typically produced a large number of hits in the forward direction and only a few in the backward direction. Either using off-line analysis or the on-line trigger processor, these events were rejected based on their upstream/downstream asymmetry in the hodoscope hit distributions. The different timing of the hodoscope hits for real and background events also helped remove out-of-time backgrounds.

In the 1987 run the CTC was not installed. In the 1988-1989 run, the longer readout time of the CTC data allowed extra events without CTC information to be recorded during the CTC readout. So the hodoscope information, when CTC data was not available, was not only used in the on-line trigger but also in the off-line analysis to determine the true primary charged multiplicity ( $N_c$ ) of the  $p\bar{p}$  collisions from the number of hodoscope hits ( $N_h$ ) for pseudorapidities between  $\pm 3.25$ . As described in ref. [13], the  $N_h$  vs  $N_c$  relationship was determined by looking at the number of tracks ( $N_s$ ) seen in the spectrometer as a function of multiplicity. The greater the multiplicity of the event, the greater the chance of a track entering the spectrometer aperture. A simple Monte Carlo program produced  $N_c$  tracks plus some number of extra tracks (to simulate secondaries from particle interactions in materials) and compared to the data. The Monte Carlo  $N_h$  vs  $N_s$  was matched to the

measured  $N_h$  vs  $N_s$  by varying the percentage of secondaries. It was found that about 20% extra tracks gave a good match to the data (which is consistent with the number of background tracks, i.e. tracks not from the primary vertex, seen in the spectrometer). The resulting  $N_h$  vs  $N_c$  relationship is shown in fig. 10. The estimated error in  $N_c$  is about  $\pm 10\%$  which is sufficient for studying, for example, the average transverse momentum of charged particles vs  $N_c$  [13] and particle production vs  $N_c$  [14,15]. Also, the GEANT detector simulation program [16] was used with several event generators to find the  $N_h$  vs  $N_c$  relationship. It was consistent with the above result.

### **Acknowledgments**

We thank William Burley, Jeanne Wilson, Chuck Chizzo, Sherry Harold, Carl Lindenmeyer, and Chuck Nila of Fermilab for their efforts. We thank also Jadwiga Piekarz, Seog Oh, Denise Hurley, Victor DeCarlo and Ramsey Harcourt for their assistance, as well as all of our E735 Collaborators. This research was supported in part by DOE Contract DE-AC02-85ER40193 and Fermi National Accelerator Laboratory.

### **References**

1. Fermilab Proposal P-735 (1983), L. J. Gutay, spokesman.
2. J. D. Bjorken, Phys. Rev. D27, (1983) 140.
3. C. Hojvat et al., to be submitted to Nucl. Instr. Meth.
4. S. Bannerjee et. al., Nucl. Instr. Meth., Phys. Res. Sect. A269, 1211(1988).
5. Harshaw Chemical Co. LiF TLDs were used and calibrated with a  $^{130}\text{mCu}$   $^{137}\text{Cs}$  source. Corrections were made for nonlinearity at high doses.
6. Model E12P45, Eagle Magnetic Co., P.O B. 24283, 7421 Crawfordsville Rd., Indianapolis, In. 46224, U.S.A.
7. Hamamatsu Corp., 429 South Av., Middlesex, N. J. 08846, U.S.A.
8. Model PSC-2-1, Mini-Circuits, P.O.B. 500, Brooklyn, N.Y. 11235, U.S.A.
9. C. S. Lindsey et al., Nucl. Instr. and Meth. A254 (1987) 212-214.
10. Bicron Corp., 12345 Kinsman Rd. Newbury, Ohio 44065, U.S.A.
11. PCS-200 Polymer Clad Silica Fiber, Fibres Optiques Ind. of France.
12. G. H. Siegel et al., IEEE Nuc. Sci. NS-26, No.6, Dec. 1979, pp.4796-4801.

13. T. Alexopoulos et al., Phys. Rev. Lett. 60:1622, 1988.
  14. S. Bannerjee et al., Phys. Rev. Lett. 62:12, 1989.
  15. T. Alexopoulos et al., Phys. Rev. Lett. 64:991, 1990.
  16. R. Brun et al., "GEANT3 Users Guide", CERN DD/EF/84-1.
- \* Present address: E735, MS-219, Fermilab, P. O. Box 500, Batavia, IL. 60555.
- \*\* Operated by the Universities Research Association, Inc. under contract with the U. S. Dept. of Energy.

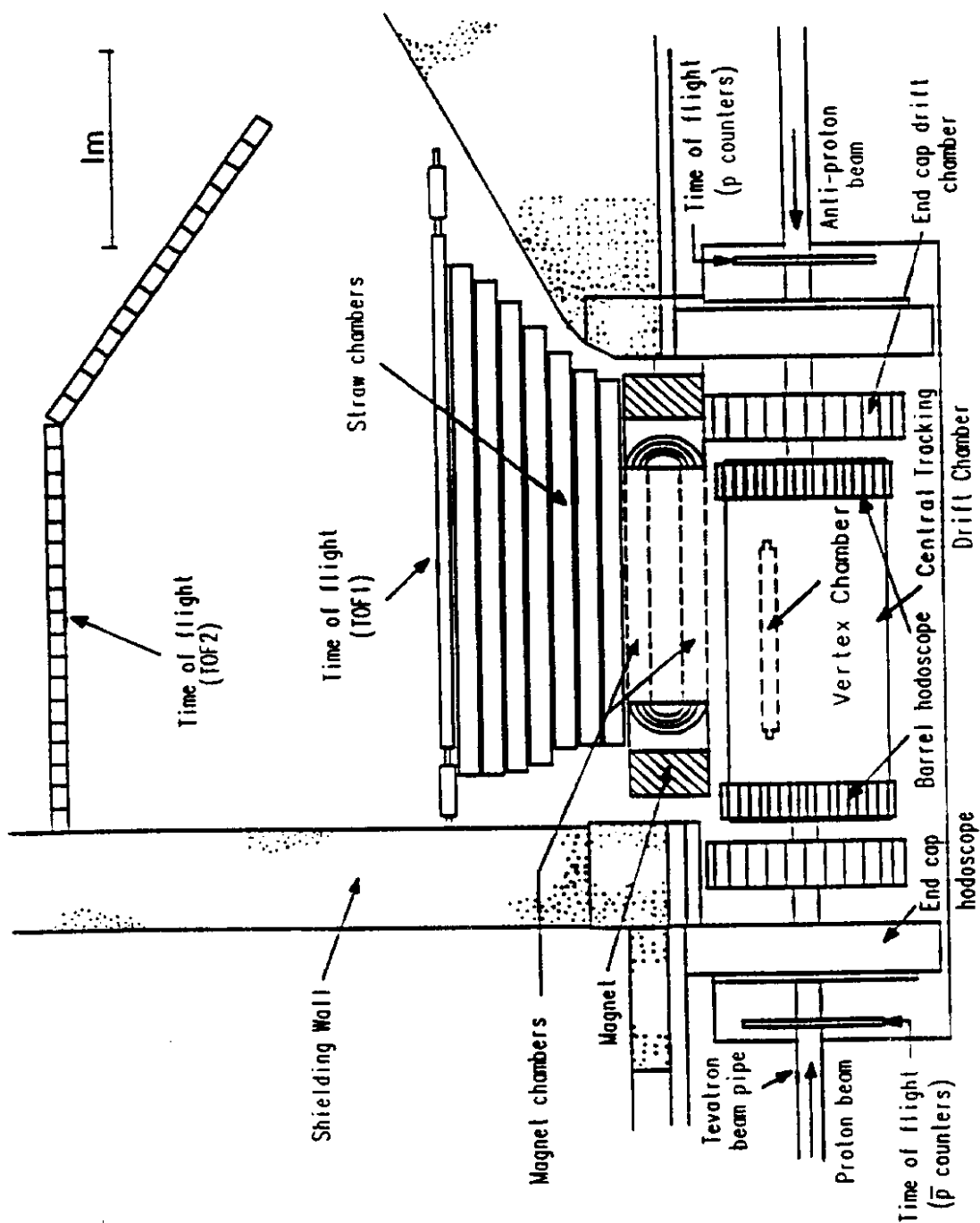


Figure 1a. Plan view of experiment E735 at the C0-intersection region.

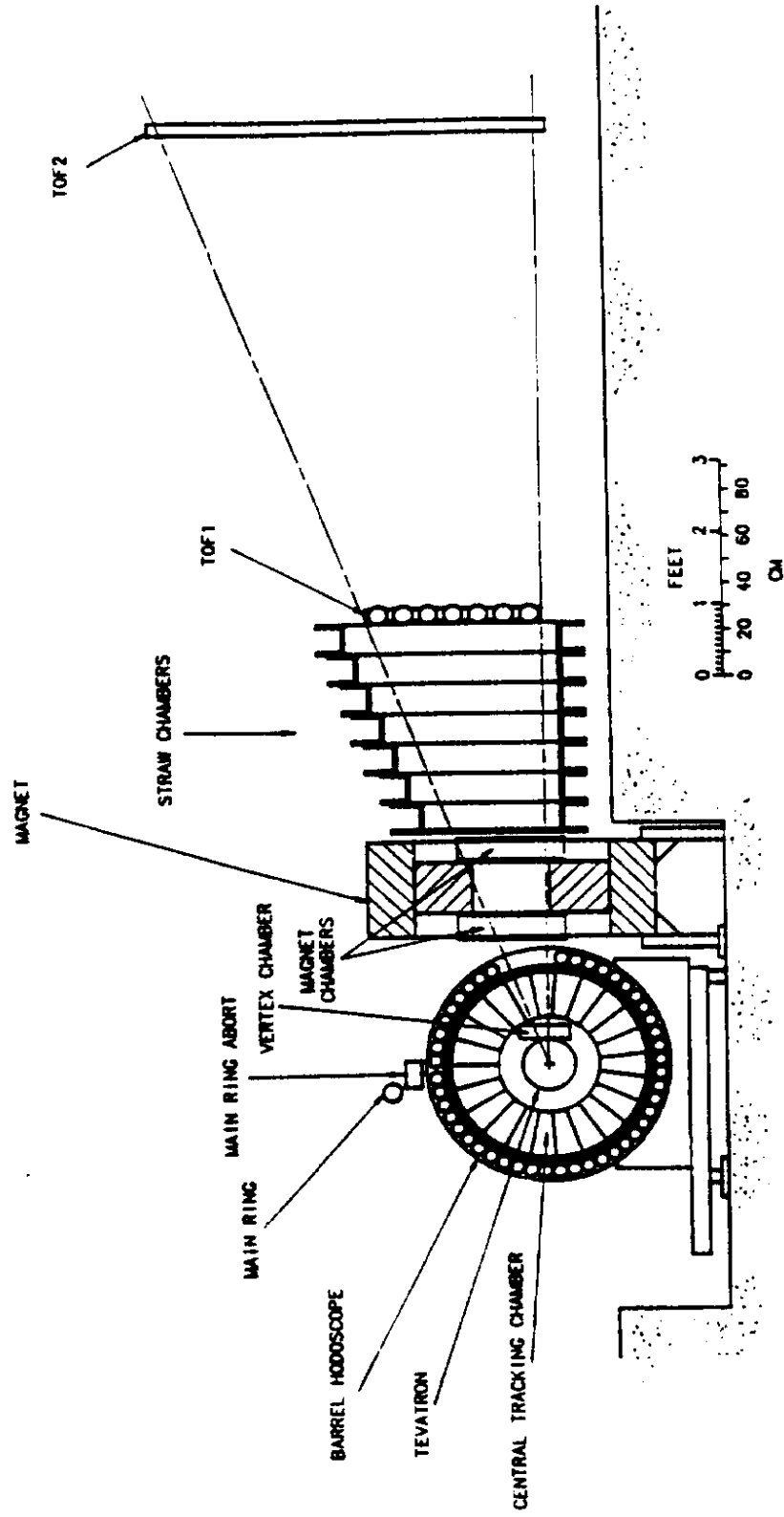


Figure 1b. Side view of E735 Detector

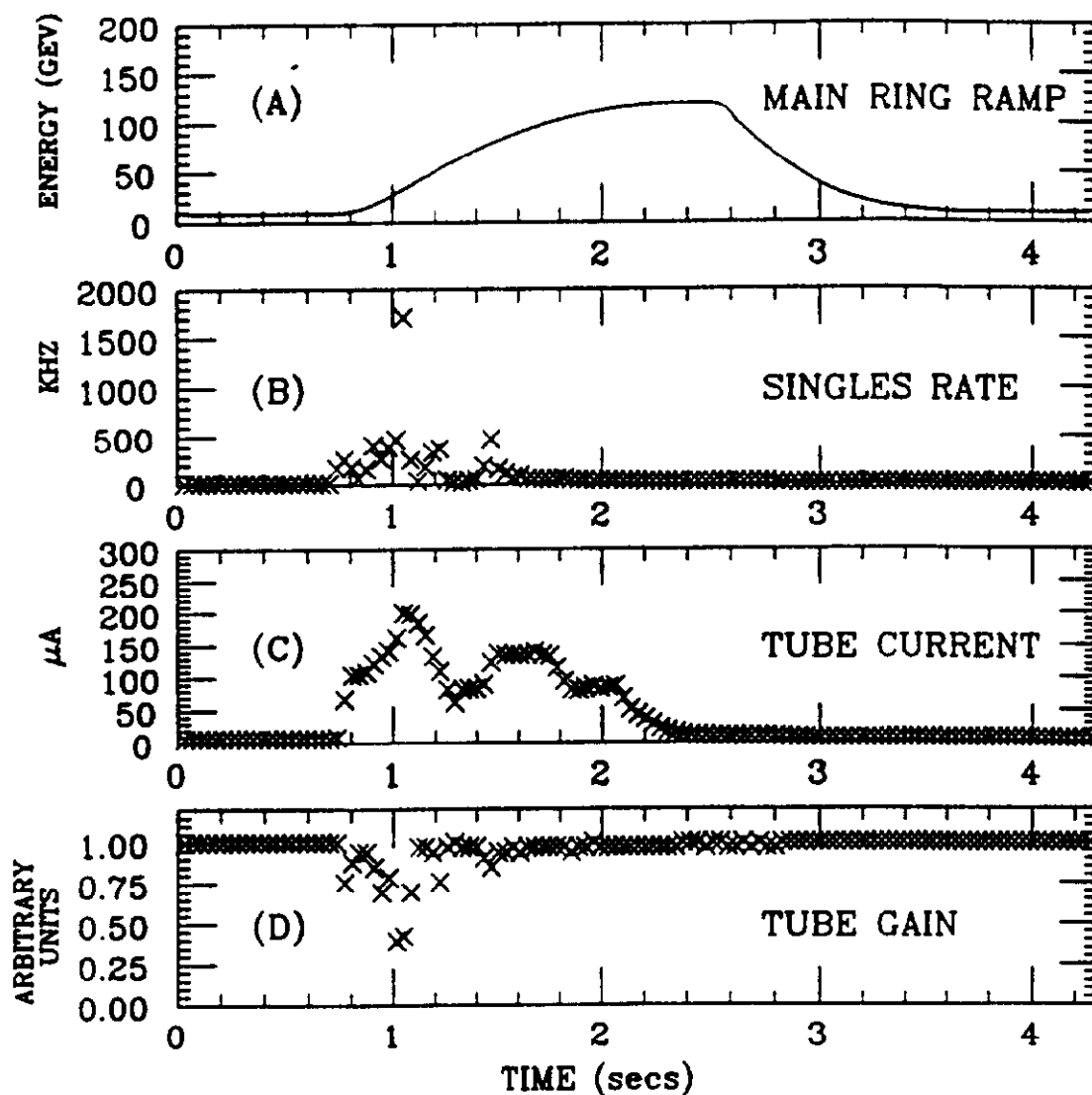


Figure 2. The Main Ring cycle showing (a) acceleration from 8GeV up to 120GeV, where protons are extracted, and back down to 8GeV; (b) hit rates in a counter with a high rate transistor base; (c) anode current for the low current base (see fig. 7); (d) photomultiplier tube gain with the low current base.

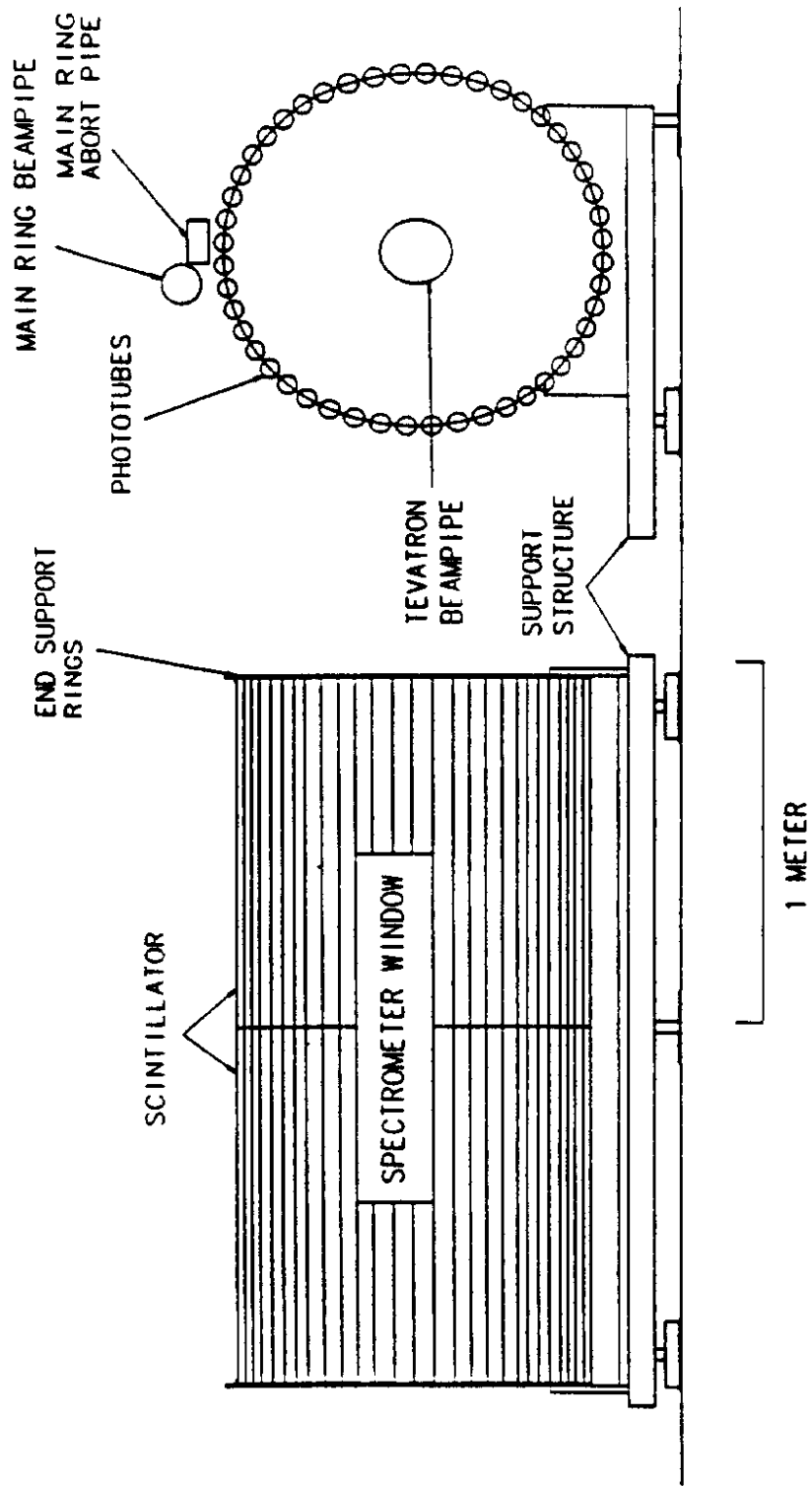


Figure 3. Barrel hodoscope side and end view.

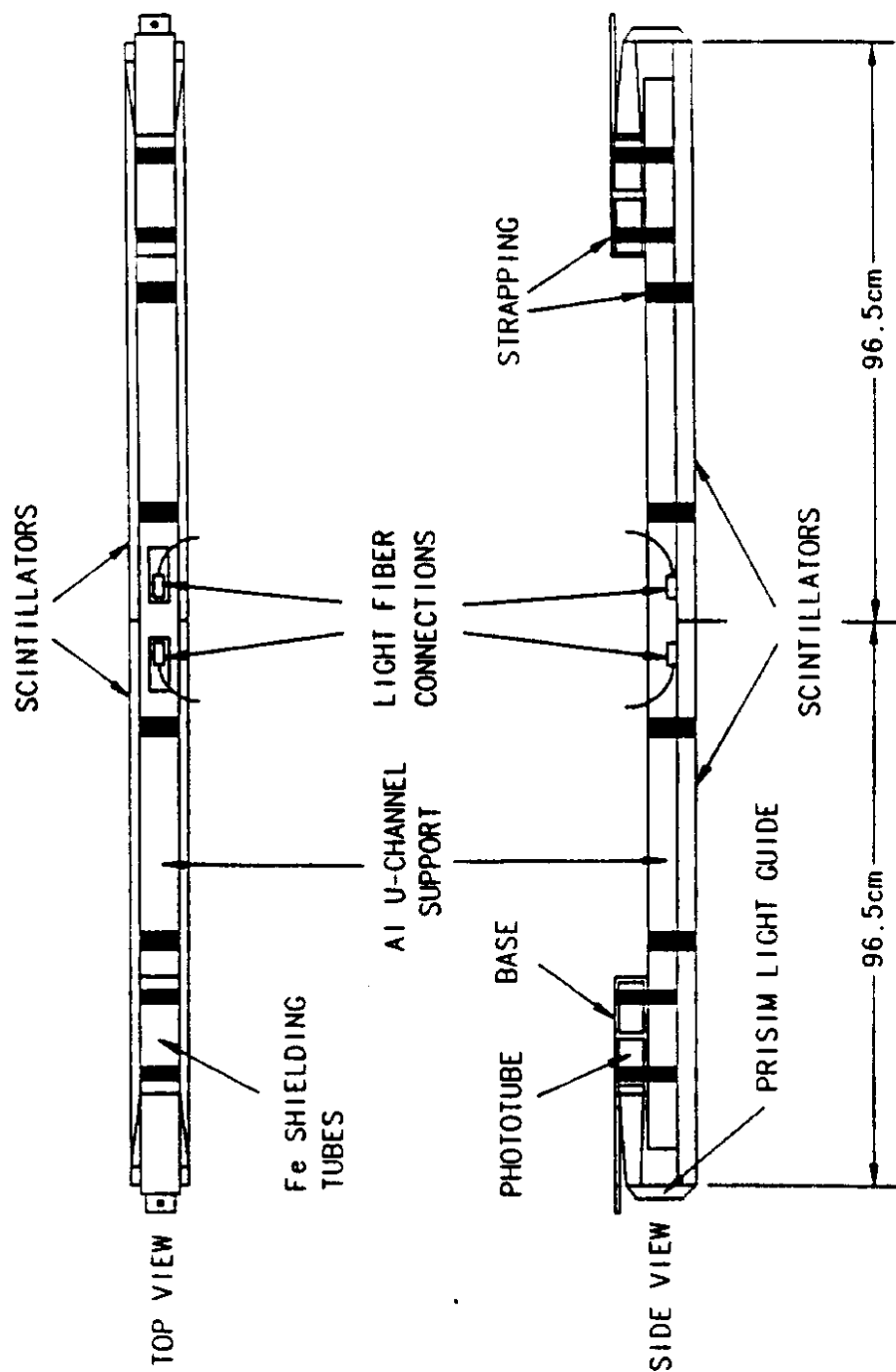


Figure 4. A barrel counter assembly.



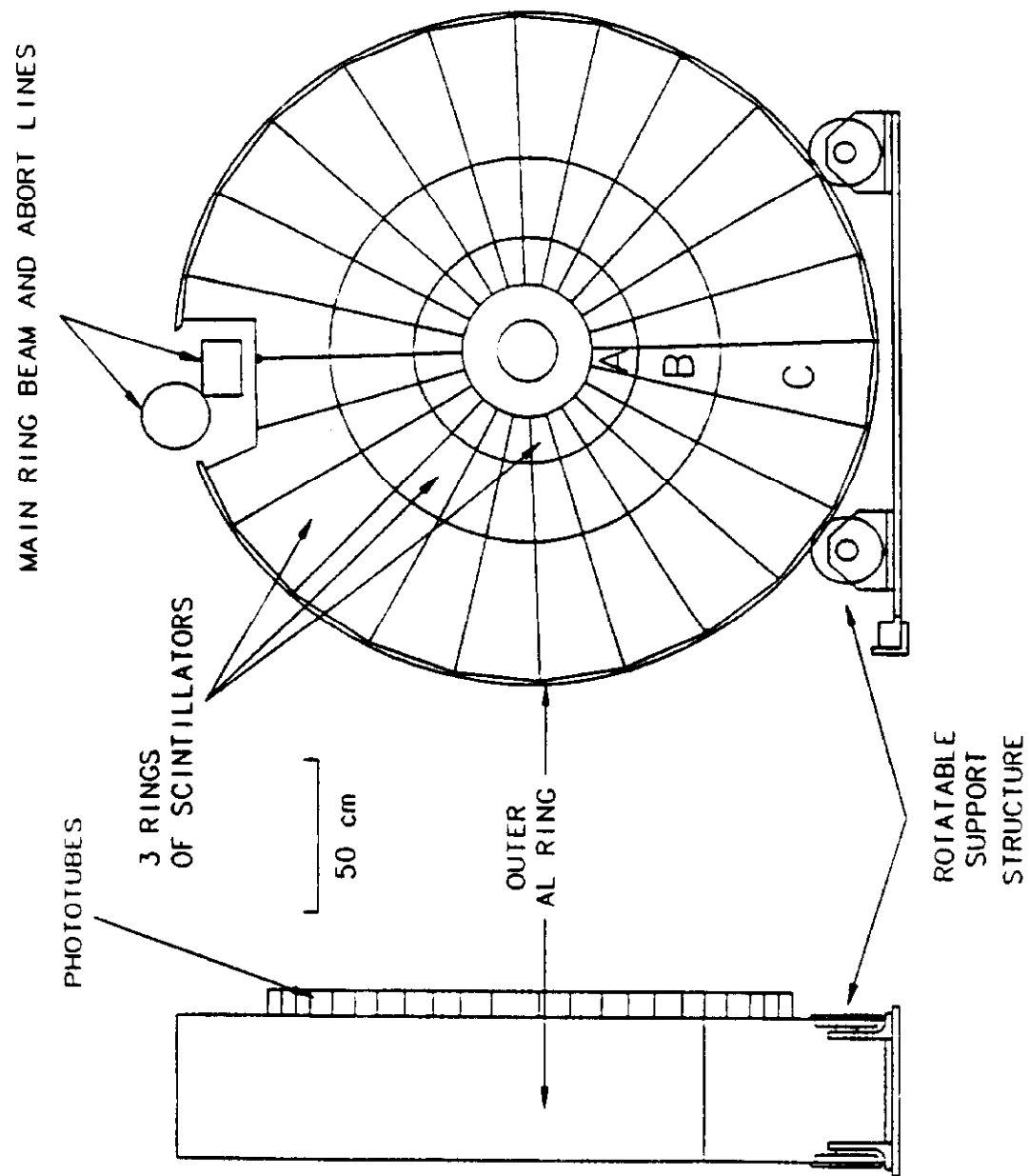


Figure 5. Endcap hodoscope side and end view.

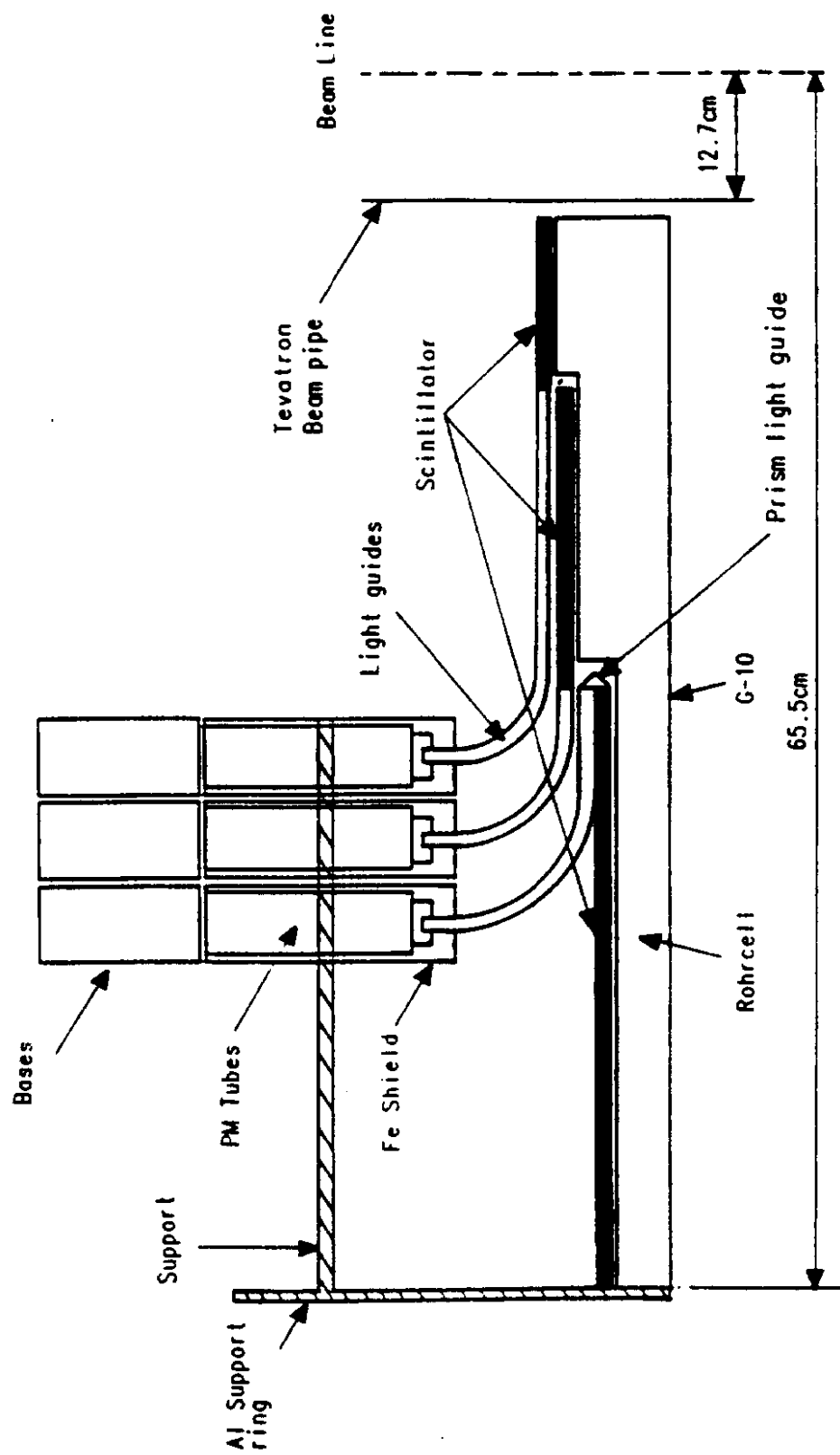


Figure 6. A cutaway of the endcap showing a side view of the three types of counters.



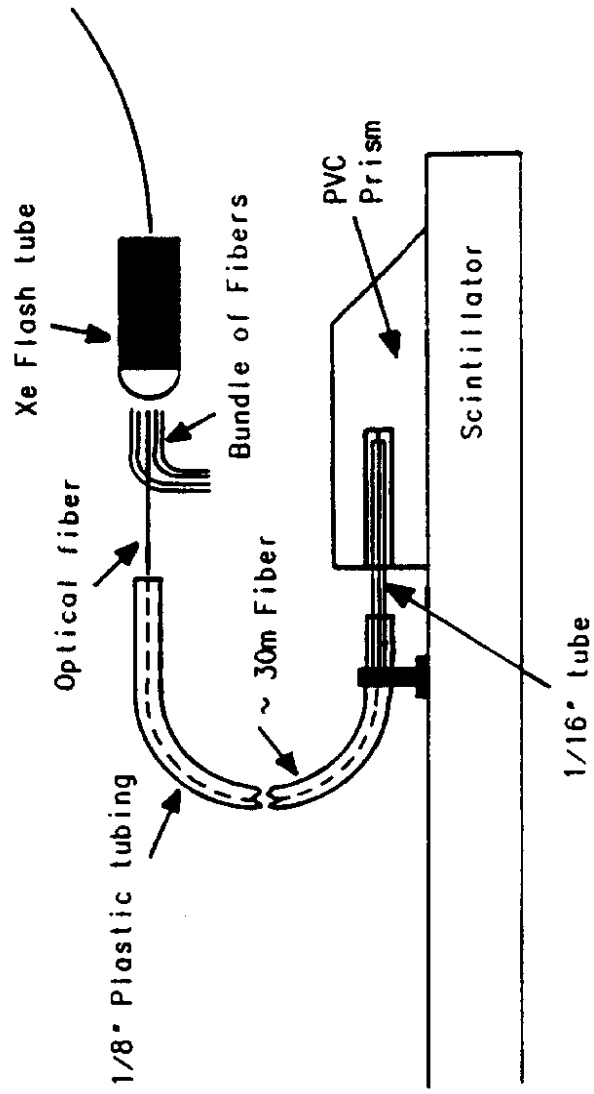


Figure 8. Light-pulser and optical fiber system for monitoring the counters.

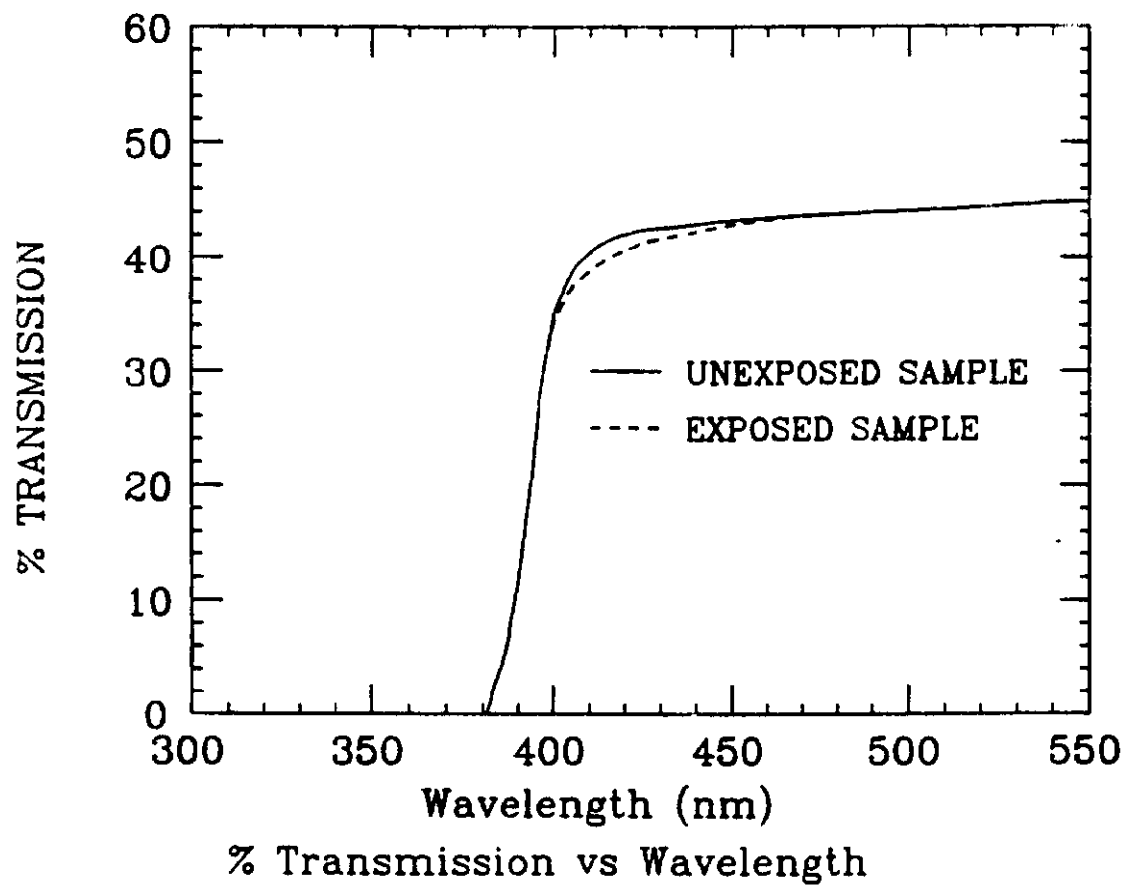


Figure 9. Transmission (relative to air) vs wavelength for 2.54cm PVT lightguide material exposed and unexposed to 25krad during the 1987 run.

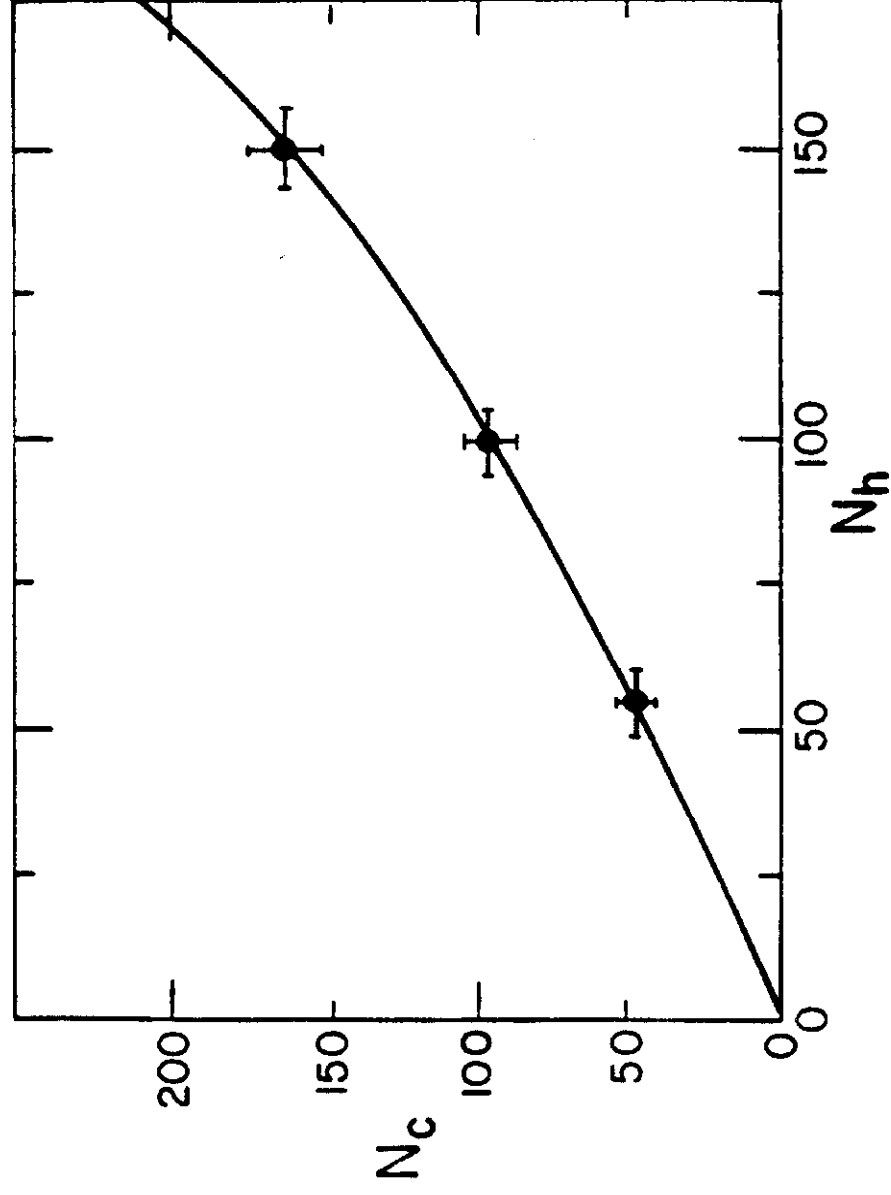


Figure 10. Number of hodoscope hits ( $N_h$ ) vs number of charged primary particles ( $N_c$ ) for pseudorapidity  $|\eta| < 3.25$  [13].